

Chapter 2

Introduction to Coherence

In any imaging system, one of the component that decides the signal to noise ratio and consequently the image quality (sharpness of the reconstructed image in holography) is the light source that is being used to image the object under investigation [98]. There are various parameters associated with the source of light such as its intensity [40,163,164], polarization [40,165] and coherence [98,166] that affects the image quality.

Illumination coherence has a particularly important implication in imaging systems in areas such as ultrasound imaging [167], telescope [168], interferometry [169], and biological and industrial applications [170]. Numerous application in optics such as optical microscopy [171], speckle metrology [172], interferometric imaging [173], holography [174], optical coherence tomography [175], quantitative phase imaging [2,176], and optical diffraction tomography [177] have been found to be influenced by the degree of coherence of the light source used. Even though light source such as laser having a high coherent illumination ensures high radiance, well-defined wavelength, and phase extraction via interferometry, it inevitably suffers from several drawbacks such as undesired diffraction effects called speckle noise or parasitic fringe. These occur due to the interference of randomly varying optical field of waves because of undesirable diffraction resulting from dust particles, imperfect optical alignment, multiple reflections etc. [101].

The three major limitations faced while performing holographic phase microscopy when using coherent light source are: poor spatial resolution, weak depth sectioning and fixed pattern noise [110]. As discussed in the previous chapter, several studies have been conducted, that shows the use low coherent sources in either spatial [103] or temporal [178] domain might lead to betterment in the image quality mainly by reducing speckle noise.

In interferometry, coherence plays a rather critical role in the generation of interference fringes. As discusses in chapter 1, the work in the thesis focuses on utilizing a low coherent source (LED) for performing interferometric as well as non-interferometric techniques. The spatial coherence of LED is engineered in order to utilize it as the source of illumination in various techniques. Therefore, before proceeding to the applications where LED has been used in

various geometries for extracting phase information of the objects under investigation, the concept of coherence is briefly discussed in the following section.

2.1 Coherence

The technique of holography majorly depends on phenomenon of interference (for recording hologram) and diffraction (for reconstructing hologram) [66]. The fundamental requirement to obtain interference fringes is that the phases of the interfering beams need be correlated in a certain way [66,67]. However, certain kind of randomness is introduced in light when unpredictable fluctuations are owing either to the source itself or to the medium (due to scattering) through which the light propagates results. For example, the light emitted by an incandescent object where the resultant light is the superposition of emissions from a large number of atoms that radiate independently giving rise to randomness [179]. These distortions arising in the wavefront need to be quantified and for that an account of correlation between different regions of the wavefront at different instances of time must be made. This correlation property associated with the light is termed as coherence.

Broadly speaking, there are two aspects to coherence: one defines the correlation of a wave with itself at various time instants, and the other defines the association of a wave with itself at all times [180] has two aspects associated to it, one that describes the correlation of a wave with itself at different instances termed as temporal coherence [98,174] whereas the one that represents the mutual coherence of different parts of the same wavefront termed as spatial coherence [98,181]. As study of fluctuations of wavefront is involved in understanding coherence of light, one has to deal with statistical behaviour of the light.

2.1.1 Temporal Coherence

To understand the concept of temporal coherence, consider the fluctuations associated to a stationary light that is fixed at one position r as a function of time. The r dependence can be dropped thus the random function transforms from $U(r,t)$ to $U(t)$ since it is assumed that the light source is fixed. The random fluctuations can be characterized by a time scale which can be considered to be the “memory” of the random fluctuations. When the time interval associated with points corresponding to fluctuations at different time instances become longer than the coherence time, the fluctuations become independent and thus the process is not able to recognize itself. Thus, a function can appear smooth in the vicinity of memory time whereas as the same function may seem erratic when studied over a long period of time. To quantify this temporal behavior a statistical average known as the autocorrelation function is employed.

This function gives a measure of the extent to which the wavefront fluctuates at the same time at two different time instances. As a result, temporal coherence refers to a wave's "correlation" with itself at different points in time as it propagates [174,182,183].

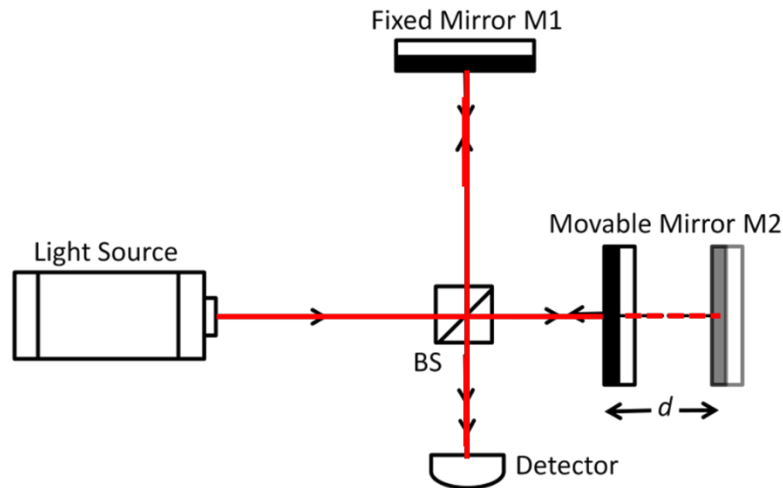


Fig 2. 1 Michelson interferometer

To understand it further, a Michelson Interferometer can be utilized as shown in Fig 2.1. A beam splitter (BS) is utilized to split the incoming beam from the light source into two waves. One beam is reflected in the orthogonal direction while the other passes through the BS and maintains the original direction. This type of splitting of light comes under amplitude division. After reflection from the mirrors M1 and M2 respectively these waves superpose at the screen (detector) after encountering the BS again [66]. For mathematical simplicity, we assume that the BS is a 50-50 beam splitter, which means it reflects half of the incoming light and transmits the other half [174]. The mutually time shifted sections of the wavefronts are superposed, in other words a portion of the beam and a slightly delayed version of its own are superposed. This time shift can be changed by axially varying the mirror's position. In the Twyman-Green arrangement (Michelson interferometer with collimated point source) the mirrors are put perfectly orthogonal to each other and a constant intensity over the screen is observed. By providing a slight tilt to one of the mirrors around one axis, interference pattern parallel to this axis can be observed. Scanning through the axial dimension will also give information about the temporal coherence.

Let the waves from mirrors M1 and M2 be E_1 and E_2 respectively where,

$$E_2(t) = E_1(t + \tau) \text{ or } E_1(t) = E_2(t - \tau) \text{ and } \tau = \frac{2d}{c} \quad (2.1)$$

The factor of “2” arises from the forward and backward propagation of light owing to the Michelson interferometer geometry. At the observation point the resulting superposition is

$$E(t) = E_1(t) + E_2(t) = E_1(t) + E_1(t + \tau)$$

and the intensity is

$$I = \langle EE^* \rangle = \langle E_1 E_1^* \rangle + \langle E_2 E_2^* \rangle + \langle E_2 E_1^* \rangle + \langle E_1 E_2^* \rangle = 2I_1 + 2 \operatorname{Re} \left(\langle E_1 E_2^* \rangle \right) \quad (2.2)$$

Eq. (2.2) results as a 50:50 beam splitter is assumed.

The complex *self-coherence* $\Gamma(\tau)$ is defined as

$$\Gamma(\tau) = \langle E_1^* E_1(t + \tau) \rangle = \lim_{T_m \rightarrow \infty} \frac{1}{T_m} \int_{-T_m/2}^{T_m/2} E_1^*(t) E_1(t + \tau) dt \quad (2.3)$$

Above equation describes the autocorrelation of $E_1(t)$. The normalized quantity

$$\gamma(\tau) = \frac{\Gamma(\tau)}{\Gamma(0)} \quad (2.4)$$

describes the coherence degree.

Since $\Gamma(0) = I_1$ is real and is the maximum value of $|\Gamma(\tau)|$, this leads to

$$|\gamma(\tau)| \leq 1$$

and

$$I(\tau) = 2I_1(1 + \operatorname{Re} \gamma(\tau)) \quad (2.5)$$

The degree of coherence cannot be directly measured, but it can be noted that for the contrast of the fringe pattern V , we have

$$V(\tau) = |\gamma(\tau)| \quad (2.6)$$

Contrast or visibility of the interference pattern is determined by [184]

$$V = \frac{I_{\max} - I_{\min}}{I_{\max} + I_{\min}} \quad (2.7)$$

Thus, for the case of an ideal coherent light, $\gamma(\tau) = 1$, emitted by a stabilized single-mode laser with infinite coherence length. For an incoherent light $\gamma(\tau) = 0$ (which is also an ideal case with coherence length=0), while partially coherent light corresponds to $0 < |\gamma(\tau)| < 1$ condition, where for all $\tau \neq 0$ we have a statistically fluctuating phase. The contrast $V(\tau)$ decreases monotonically with τ . The coherence time (τ_c) is given as the shift in time at which the contrast is reduced to $1/e$ [184]. The degree of coherence in a spatial (along the propagation direction of a light beam) domain is quantified by coherence length [185]. Coherence time is computed by measuring the contrast as a function of optical path difference in interferometers and the coherence length is defined by

$$l_c = c\tau_c \quad (2.8)$$

If the contrast function is periodic rather than monotonically decreasing (as in a two-mode laser), the coherence time refers to the time shift corresponding to the first minimum [174].

The important aspect of the source on which the temporal coherence depends is the spectral width or the line width of the source (purity of the source). An electromagnetic wave having infinite length does not exist in real world and in all practical light sources, they are emitted in wave trains or wave packets. The lengths of the trains or packets are finite due to fact that the atom does not emit a single frequency but a spectrum of frequencies (spectral width) which become broader as the lengths of the wave trains becomes shorter [186]. The spectral profile determines the relationship between coherence time and spectral width [179] as shown in the table below.

Spectral Density	Spectral Width $\Delta\nu_{FWHM}$ (Hz)	Spectral Width (nm)
Rectangular	$\frac{1}{\tau_c}$	$\frac{c(\Delta\lambda)}{\lambda_1\lambda_2}$
Lorentzian	$\frac{1}{\pi\tau_c} \approx \frac{0.32}{\tau_c}$	$0.32 \frac{c(\Delta\lambda)}{\lambda_1\lambda_2}$
Gaussian	$\frac{(2\ln 2/\pi)^{1/2}}{\tau_c} \approx \frac{0.66}{\tau_c}$	$0.66 \frac{c(\Delta\lambda)}{\lambda_1\lambda_2}$

It can be seen from the definition that,

$$\Delta\nu_c \propto \frac{1}{\tau_c} \quad (2.9)$$

regardless of the spectral profile [179]. Thus, temporal coherence provides the idea about the spectral purity of the source i.e. light from a narrow band source has the high degree of temporal coherence whereas light from a broadband source has a low temporal coherence.

2.1.2 Spatial Coherence

Correlation of different regions of the same wavefront defines the spatial coherence of the source, which can be explained with the help of Young's double aperture interferometer (shown in Fig 2.2). A wavefront-division interferometer is a type of interferometer in which two geometrically different parts of same wave superpose to produce a fringe pattern (under certain conditions). As shown in the Fig 2.2, light from an extended source, that can be considered as a distribution of large number of point sources, is allowed to fall on an opaque

screen containing two apertures or parallel slits with a separation of d [174]. Light rays take different routes to reach the screen, by either passing through the upper or the lower aperture, thereby giving rise to interference fringes [187]. If the distance between the apertures exceeds the critical limit, the interference pattern ceases to exist. This limit is named as *coherence distance* [66].

The reason for limited coherence distance is as follows: Light from different point sources on the extended light source superimpose on the screen. A situation may arise where a particular point source generates an interference maximum at a point on the screen while another point source generates an interference minimum at the same point on the screen. The reason for this situation is the fact that light from different point sources travel along different path and different distances to reach the screen. This is how the contributions from all point sources compensate themselves and the contrast vanishes.

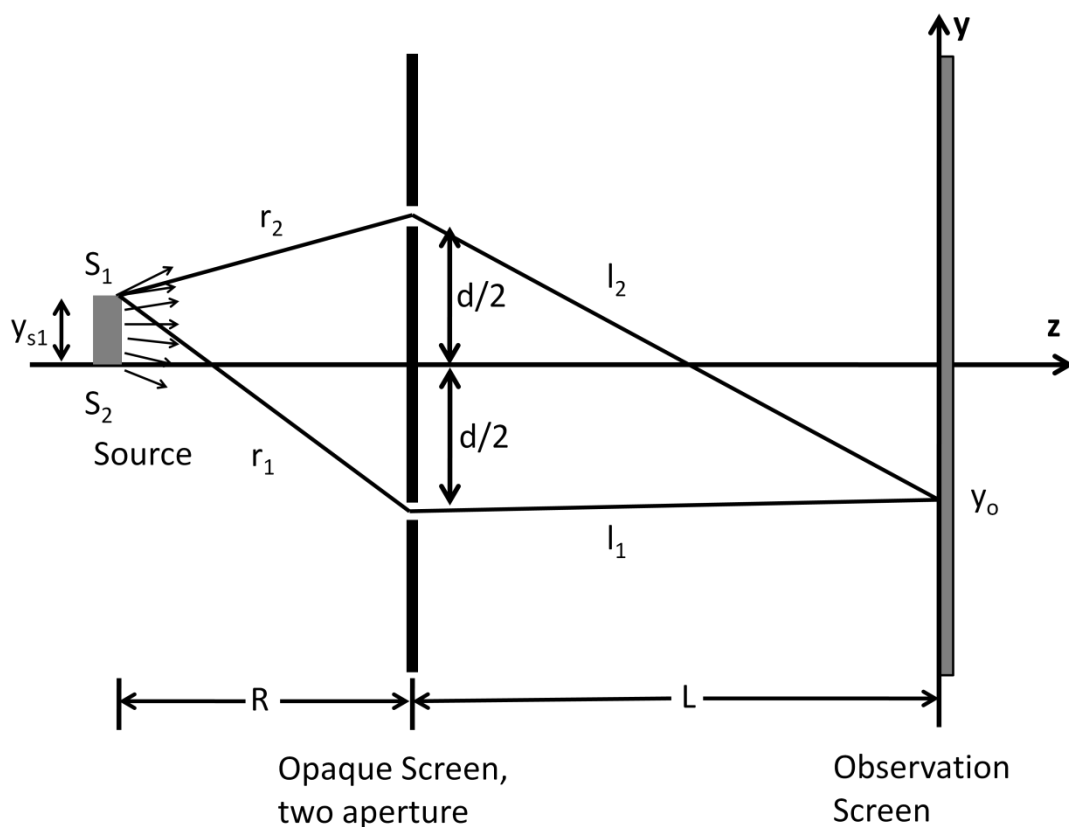


Fig 2. 2 Young's double slit interferometer

Let $S_I=(0, Y_{SI}, -R-L)$ be a single point source of extended light placed behind the opaque screen containing two apertures at a distance R . Only the light passing through the apertures contribute to the interference pattern which is obtained on the detector/observation screen kept at a distance L from the screen containing apertures. Let r_1, r_2 be the distance from S_I to the two

apertures respectively and let l_1, l_2 be the distance of the two apertures from the observation point on the screen.

Assuming the intensities of the two spherical wavefronts leaving the two apertures to be equal, the intensity at the observation screen is given by

$$I(x, y) = I_1 + I_2 + 2\sqrt{I_1 I_2} \cos^2 \Delta\phi(x, y), \text{ where } I_1 = I_2 = I_o$$

$$I(x, y) = 4I_o(x, y) \cos^2 \Delta\phi(x, y) \quad (2.10)$$

The half phase difference $\Delta\phi$ is given by

$$\Delta\phi = \frac{1}{2} \left(\frac{2\pi}{\lambda} \Delta l \right) \quad (2.11)$$

where Δl is the distance between the source S1 and the observation point at $B=(0, Y_0, 0)$

$$\Delta l = r_2 + l_2 - r_1 - l_1 \quad (2.12)$$

By substituting the values of r_1, r_2, l_1, l_2 simplifying and approximating $\sqrt{(1 + b)}$ to $1 + b/2$ and we get

$$\Delta l = -d \left(\frac{y_{s1}}{R} + \frac{y_o}{L} \right) \quad (2.13)$$

Now the resulting irradiance is proportional to

$$I = I_o \cos^2 \left[\frac{\pi d}{\lambda} \left(\frac{y_{s1}}{R} + \frac{y_o}{L} \right) \right] \quad (2.14)$$

which represents a fringe pattern with a spacing of parallel to the x-axis. $\lambda L/d$ in the y-direction.

Let S2 be a second point source on the optical axis that emits a spherical wave with equal phase that reaches the apertures, resulting in maximum intensity where the optical axis intersects the observation screen. The light from point source S1, on the other hand, produces a fringe system that is shifted laterally due to the fact that r_1 and r_2 are not of equal length. As a result, the phase difference in the two spherical waves that emerge from the two apertures is

$$\phi_1 - \phi_2 = \frac{2\pi}{\lambda} (r_1 - r_2) \quad (2.15)$$

resulting in the lateral shift of the interference pattern by an amount of

$$\Delta y = \frac{L}{d} (r_1 - r_2) \quad (2.16)$$

Simultaneous emission from S1 and S2 will produce a consistent interference pattern that is identical to that obtained from a single point source if S1 and S2 have a fixed phase relationship.

If the phase between S1 and S2 fluctuates randomly, however, the resultant is the sum of the intensities. As a result, a lateral shift of less than half fringe spacing can be set as a condition for fringe visibility.

$$|\Delta y| < \frac{1}{2} \left(\frac{\lambda L}{d} \right) \text{ or } |r_1 - r_2| < \lambda/2 \quad (2.17)$$

But we know that $|r_1 - r_2| = dl/R$ and thus we have $dl/R < \lambda/2$

As the derivation is carried out for the two furthest points S_1 and S_2 of the extended source the condition is valid for rest of the points.

The path lengths from the aperture to the observation screen are nearly identical near the optical axis. There, the fringe pattern informs us about the wavefront $E(r_1, t)$ and $E(r_2, t)$ similarity at the apertures r_1 and r_2 without time shift. The *spatial coherence function* can express this similarity.

$$\Gamma(r_1, r_2, 0) = \Gamma_{12}(0) = \langle E(r_1, t) E^*(r_2, t) \rangle \quad (2.18)$$

The general spatio-temporal coherence function now is

$$\Gamma(r_1, r_2, t_1, t_2) = \Gamma_{12}(t_2 - t_1) = \Gamma_{12}(\tau) = \langle E(r_1, t + \tau) E^*(r_2, t) \rangle \quad (2.19)$$

which can be normalized to give the mutual degree of coherence

$$\gamma_{12}(\tau) = \frac{\Gamma_{12}(\tau)}{\sqrt{\Gamma_{11}(0)\Gamma_{22}(0)}} \quad (2.20)$$

Where $\Gamma_{11}(0)$ is the intensity at r_1 , $\Gamma_{22}(0)$ is the intensity at r_2

The spatial coherence of thermal discharge sources is mainly determined by the source's spatial extent. R becomes very large at long distances from the source, satisfying the condition $dl/R < \lambda/2$. So, on the earth (at a great distance from Earth), we receive coherent light from stars and other large thermal terrestrial sources, which is used in the field of stellar interferometry. This demonstrates that coherence is a property of the light wave, not the source.

The transverse mode structure of the resonance cavity is linked to the spatial coherence of laser light used in holographic interferometry. All points on the wavefront of lasers resonating in the TEM₀₀ mode have essentially the same phase, resulting in extremely high spatial coherence. [174].

Following image (Fig 2.3) summarizes pictorially both temporal and spatial coherence in case of a plane waves.

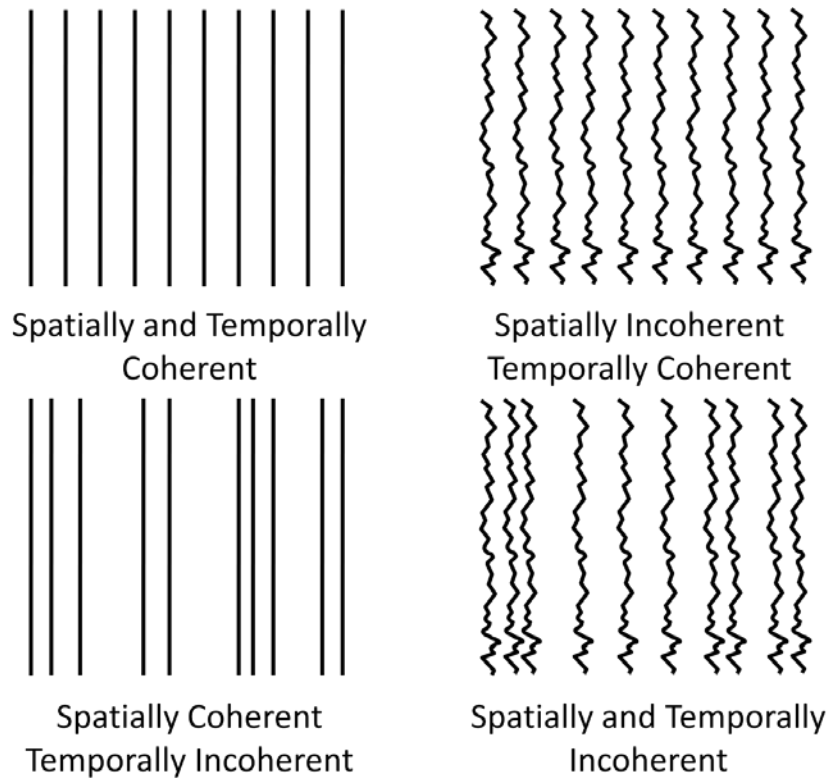


Fig 2. 3 Pictorial representation of temporal and spatial coherence in the case of plane waves

In the last few decades, the technical progress in the field of low coherent, high brightness light emitting diodes (LEDs) has been spectacular [188]. There has been an extraordinary progress in LED efficiency, life-time, and total lumen output [189]. State of the art LEDs which are small, rugged, bright and with high efficiency have been developed and because of their potential applications in general illumination, traffic light signals, the automobile industry, machine vision systems, and display technologies, LEDs are becoming increasingly important. [188–193].

The low spatiotemporal coherence of the LED reduces the effect of speckle in the images thereby improving the signal to noise ratio which makes them well suitable for performing low coherence interferometry, profilometry, microscopy and digital holography especially in the areas of biomedical imaging and diagnosis [117,190].

However, owing to their low spatiotemporal coherence, it becomes difficult to generate high contrast interference fringes over a large FOV [129]. In the following chapters, we have made use of LED as an illuminating source in imaging system wherein its properties such as intensity, spatial coherence and temporal coherence (line width), have been exploited in non-interferometric (Fringe Projection technique) and interferometric techniques (digital

holographic microscopy) to retrieve phase information of objects such as human RBCs. Further, we have also performed Optical coherence tomography by utilizing LED as the light source instead of Super luminescent diode which are used conventionally in performing OCT along with a webcam sensor to make the system compact and cost effective.